Effect of the external electric field on surface states: An *ab initio* study

P. A. Ignatiev and V. S. Stepanyuk*
Max-Planck-Institut für Mikrostrukturphysik Weinberg 2, D-06120 Halle, Germany
(Received 5 April 2011; revised manuscript received 20 May 2011; published 5 August 2011)

Here we present an *ab initio* study of surface states exposed to an external electric field. We demonstrate that the external electric field affects both the vacuum decay rates and the dispersion relations of surface states. In particular, the Cu(111) surface-state band bottom is shifted by means of the external electric field. Spin-selective screening of spin-polarized surface states on a Co bilayer on Cu(111) leads to the possibility of reversing the sign of the surface-state spin polarization.

DOI: 10.1103/PhysRevB.84.075421 PACS number(s): 71.15.Mb, 73.20.At

I. INTRODUCTION

Scanning tunneling microscopy and spectroscopy (STM/STS)[1] are well-developed techniques providing a unique way to acquire various properties of surfaces and adsorbates experimentally, with atomic-scale resolution. In particular, it is widely accepted that scanning tunneling spectra are proportional to the local density of states (LDOS). Theoretical grounds for this statement come from the theory by Tersoff and Hamann,[2] and strictly speaking, such a view is often oversimplified. One of the most obvious corrections concerns the fact that an STM tip itself disturbs the potential and, hence, the electronic structure of the probed sample. If a bias voltage is applied during STM measurements, then the effect of the tip becomes just stronger. The applied voltage can be accounted for in terms of the external electric field created between the tip and the sample. Any changes in the system can consequently be treated as being caused by the external electric field. It is important to note that the electric field decays more slowly than other types of interactions in the STM junction.

The importance of the electric field created in STM experiments was realized at the very beginning. Eigler and Schweizer used the applied voltage to tune the tip-induced force acting on adsorbate atoms.[3] It was demonstrated later that the tip-induced field can be exploited to initiate a directional diffusion of polarizable atoms[4] or even to create from them a new kind of surface structures.[5] Theoretical study clarified the importance of the tip shape.[6] It was shown that atomic protrusions of sharp tips confine the electric field, increasing its strength under the tip. The increased field facilitates attachment of adsorbates to the tip. At the same time, it was revealed that the applied voltage can modify structures of both the tip and the sample. For example, high-voltage pulses applied to the tip resulted in the deposition of the tip material onto the surface,[7] and electrostatic forces can be involved in manipulations with the surface structure.[8,9] Wulfhekel *et al.* have recently observed field-induced structural changes of Fe nanoislands on Cu(111) accompanied by the magnetic phase transition.[10] The applied field can also modify adsorption energies, adsorption sites,[11] and govern kinetics of surface diffusion of adsorbates.[12,13]

Field-induced changes of surface structure, adsorption energies, and diffusion kinetics are caused by a redistribution of electron density. This statement was unambiguously illustrated by means of theoretical *ab initio* studies.[13–16] Theory also predicted the possibility to increase magnetism by means of the external electric field.[17,18] Similar effects were found experimentally.[19,20] The external field can be used to change magnetocrystalline anisotropy.[21–23] Recently, theoretical investigations predicted the possibility of switching the magnetic states in multistable magnetic nanostructures by means of the external electric field.[24]

Direct observations of field-induced shifts of surface-related electronic structure have been reported in several recent papers.[25–27] All these studies were performed by means of STM/STS on various noble metal substrates. Attention was focused on surface-localized electronic states, namely, on the Shockley-type surface state[25,26] and on image potential states.[27] In all cases, STS clearly showed dependence of the binding energy of surface-localized states on the electric field created by the STM tip. Obtained results were explained in terms of either simple quantum-mechanical models or by means of a semiempirical surface potential.[26]

In this paper we present an *ab initio* study of the effect of the external electric field on the surface states. Self-consistent calculations are performed by means of the Korringa-Kohn-Rostoker (KKR) Green's function method supplemented with the possibility of introducing an external electric field. First, we apply our method to the surface state of Cu(111) and then we proceed to spin-polarized surface states on a Co bilayer on Cu(111). The rest of the paper is organized as follows. In Sec. II we present the method used. We point out conceptual changes from the field treatment in the supercell codes and show how the external electric field can be introduced in the KKR. Section III is devoted to our results on the effect of the external electric field on surface states. Our method is used to explain recent experimental results on the Stark shift of the Shockley surface state on Cu(111)[26] and then is applied to spin-polarized surface states on Co bilayers on Cu(111). Results are accompanied by discussions.

II. METHODS APPLIED

A. Field in supercell geometries

Plenty of *ab initio* codes deal with three-dimensional (3D) periodicity. Systems in such codes are described by means of supercells periodically repeated in three dimensions. The Kohn-Sham effective potential $v_{\text{eff}}(\mathbf{r})$ describing quasiparticles of a 3D periodical system must also be periodical with respect to superlattice vectors $\mathbf{G}_n$: $v_{\text{eff}}(\mathbf{r}) = v_{\text{eff}}(\mathbf{r} + \mathbf{G}_n)$. Potential

$V_{ext}(\mathbf{r})$, describing the external electric field $\mathbf{E} = -\nabla V_{ext}(\mathbf{r})$, is incorporated in $v_{eff}(\mathbf{r})$ and is also periodic. The most obvious physically relevant system described in this manner is a surface modeled with a slab. The field in this case is perpendicular to the surface and the corresponding external potential is defined by means of a saw-like function.[14,15] The longer slope of the saw "tooth" crosses the slab, creating the additional electric field on its opposite sides. The shorter backward slope is introduced in the vacuum region in order to make the $U_{ext}(\mathbf{r})$ periodic. Very often such a setup is referred to as a field of artificial dipole sheets. The described approach was successfully implemented in a number of modern *ab initio* codes.[13,15,28–31]

B. Basics of the KKR method

The approach used in supercell codes cannot be applied in the KKR Green's function method. This method is based on the density functional theory (DFT). Results presented in this paper were obtained by means of the local spin density approximation (LSDA) to the exchange correlation functional. Each atom of a crystal is represented as a spherical scattering potential defined inside so-called atomic sphere. Radii of these atomic spheres are the same in all the calculations. Electronic structure is determined by solution of the Kohn-Sham equations using the multiple scattering formalism.[32] The ground state electronic density $\rho(\mathbf{r},\varepsilon)$ is expressed in the KKR by means of the self-consistent Green's function of the system as $\rho(\mathbf{r},\varepsilon) = -1/\pi\ \mathrm{Im}\, G(\mathbf{r},\mathbf{r},\varepsilon)$. The Dyson equation states a possibility to express the Green's function $\mathrm{G}(\varepsilon)$ of any perturbed system from the Green's function $\mathrm{G}_0(\varepsilon)$ of the reference system as[33,34] $\mathrm{G}(\varepsilon) = \mathrm{G}_0(\varepsilon) + \mathrm{G}_0(\varepsilon)\mathrm{V}(\varepsilon)\mathrm{G}(\varepsilon)$, where $\mathrm{V}(\varepsilon)$ is a perturbation potential. More precisely, a bulk crystal is treated as a periodic 3D perturbation of the free space. The Dyson equation in this case is formulated in the reciprocal space. A surface is considered as a 2D perturbation of the infinite bulk crystal. Atoms outside the perturbed region are considered to be the bulk ones. There are three different geometry setups suitable for surface description in the KKR: (i) a finite material slab in the vacuum; (ii) a half-infinite crystal on the one side and half-infinite vacuum on the other side; (iii) an infinite 2D vacuum slab inside a crystal. All these geometries have a 2D in-plane periodicity and simulations of the external electric field by means of the "saw-like" potential periodic in the direction perpendicular to the surface plane are impossible.

Surfaces presented in this paper were constructed using the experimental Cu lattice constant of 3.615 Å. Surfaces were unrelaxed. Additional tests performed by means of the VASP code clarified that the electric field applied in our studies does not substantially change the relaxations of surfaces. Self-consistent electronic structures of bulk crystal and surfaces were calculated using 1469 and 65 k points in the irreducible parts of the corresponding 3D and 2D Brillouin zones (IBZs), respectively. To calculate the LDOS, the density of k mesh in the 2D IBZ was increased to 884 k points.

C. Introducing an electric field in the KKR

The external electric field $\mathbf{E} = -\nabla V_{ext}(\mathbf{r})$ can be treated in the spirit of the KKR as a perturbation $V_{ext}(\mathbf{r})$ of the unbiased 2D reference system. This 2D perturbation must be bounded and confined near the surface. The latter condition means that perturbing potential must vanish at the boundary of the perturbed part of the system. Geometries i and ii are open so unbounded potential $V_{ext}(z)$ must be artificially zeroized at some distance from the slab. It can be done, for example, exploiting the concept and the theory for the effective screening medium.[35] In the third geometry, the external electric field is created inside the 2D finite vacuum region, perturbing the infinite bulk crystal. If the bulk is metallic, then the field inside the vacuum slab is screened by metal surfaces and therefore is confined inside the perturbed region. Such a description is clear and reasonable from the physical point of view; it does not require conceptual changes of the code. These arguments indicate the advantage of the surface described in the KKR by an infinite 2D vacuum slab inside a crystal.

It is still necessary to decide how the external field is introduced inside the 2D vacuum slab. The method used in supercell geometries, when the field is created by a specially constructed potential, seems rather tedious. It is much easier to generate the electric field directly by means of extra charges placed inside the vacuum slab. The density of these extra charges must not be redistributed during self-consistent calculations; they are placed just to create the electric field. Charge neutrality is achieved automatically because the chemical potential of the system is fixed to the crystal value. Extra charges must have a 2D periodicity in the surface plane. In the simplest case, point charges can be placed at centers of vacuum spheres of some layer in the perturbing region. The exact field created by such a 2D periodic system of point charges should be calculated by means of the Poisson equation formulated in terms of multipole expansion of the charge density and solved exploiting the Ewald summation technique, as has actually been done in the KKR code.[32]

D. Quantitative description of the field

The electric field created by the 2D lattice of point charges must be described quantitatively. For *ab initio* calculations with the external field, we chose two geometries. In the first system, perturbation of the bulk crystal was composed of six Cu layers, nine vacuum layers, and, again, six Cu layers. Extra charges were introduced in the middle of the vacuum slab, that is, in the fifth vacuum layer at a distance of 10.4 Å from the topmost Co layer. In the second case, the thickness of the vacuum slab was reduced to five layers and extra charges were placed in the third layer at a distance of 6.2 Å. Two systems were investigated to check the stability of results with respect to the thickness of the vacuum slab. In addition, the potential created by the external field depends linearly on the distance from the surface. The larger the distance, the deeper the attractive potential well created by positive charges. If the well is deep enough, then electrons can overcome the reduced work function of the surface and field emission starts. To reduce the depth of the potential well, one can place extra charges closer to the surface. This hint allows us to create stronger fields, avoiding field emission.

Fields fitted from the self-consistent Coulomb potentials calculated in vacuum layers are presented in Fig. 1 as a function of the extra point charge q. The sign of the field

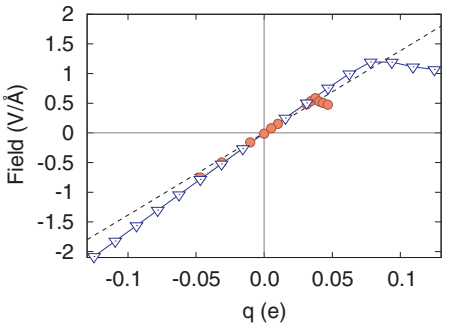

FIG. 1. (Color online) Effective electric field as a function of the generating point charge. The field strength is fitted from *ab initio* Coulomb potentials. Circles correspond to a nine-layer-thick vacuum slab with extra charges placed in the fifth layer. Triangles demonstrate results obtained for a five-layer-thick vacuum slab with extra charges in the third layer. The dashed (black) line shows the field of the uniformly charged plane.

coincides with the sign of the extra charges,[36] that is, positive and negative charges create positive and negative fields, respectively. Results obtained for extra charges placed in the fifth (10.4 Å) and third (6.24 Å) vacuum layers (plotted in Fig. 1 with circles and triangles, respectively) coincide with each other for $q < 0.0375$ e. If the point charge exceeds this critical value, then the external field reduces the work function of the surface and field emission becomes possible. In a narrower slab, field emission starts at the critical charge of about 0.078 e. The *ab initio*–fitted fields can be compared with the electric field $E = \sigma/(2\epsilon_0)$ of the infinite charged plane (σ is the charge density of the 2D unit cell). The electric field calculated by means of this approximation is shown in Fig. 1 by the dashed black line. Overall agreement between the simple theory and *ab initio*–fitted effective fields is reasonably good. Figure 1 demonstrates that the suggested method allows calculation of electric fields with a strength of up to 1 V/Å.

III. RESULTS AND DISCUSSION

A. Surface state of Cu(111)

The Shockley surface state is very often referred to as a quasi-2D free-electron-like state localized at the surface.[37,38] It arises in the projected inverted bulk band gap due to breaking of the crystal symmetry at the interface. The Shockley surface state is confined between the vacuum barrier and the projected gap of the bulk crystal electronic structure. As any bound state, the Shockley surface state decays exponentially both in vacuum and inside the crystal. It is very important for us that the density of surface-state electrons is higher above the surface than that of their bulk counterparts, an, therefore, the surface state should be more strongly affected by the external electric field. Figure 2(a) shows local densities of surface states calculated for various strengths of the external electric field within the second vacuum layer at 4 Å above the surface. The external field affects both the intensity of the surface state and the position of its band bottom. Positive fields increase the density and push the surface-state onset to lower energies, while negative fields act contrariwise. These energy shifts have recently been referred to as the Stark effect.[26]

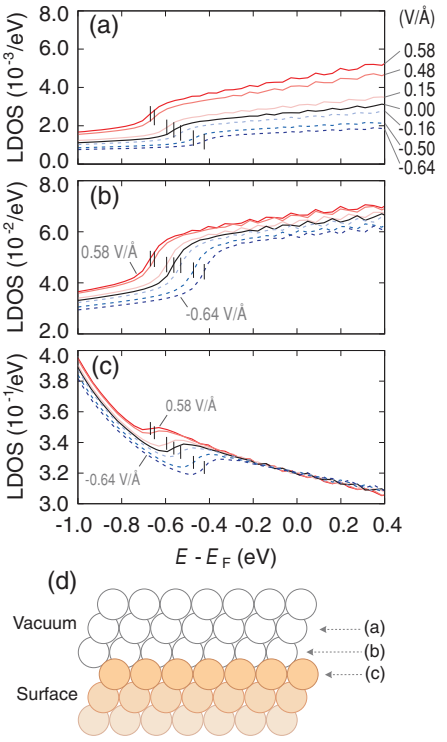

FIG. 2. (Color online) (a–c) LDOS calculated in several vacuum spheres near the Cu(111) surface as shown in (d). LDOS values obtained at positive, zero, and negative external fields are plotted by light solid, black, and light dashed curves, respectively. Corresponding field strengths are noted at the right-hand side in (a).

The external field modifies the vacuum potential confining the surface state from the outer side. Such variations of confinement conditions affect the energies of the surface state, as well as the densities of their evanescent tails tunneling into the vacuum. The negative field enhances the vacuum potential barrier. The surface state gets more confined and its band bottom shifts to higher energies. A steeper vacuum barrier hinders the spread of surface-state electrons into the vacuum, decreasing the LDOS above the surface. The positive field decreases the vacuum potential, making the surface state more free-like, increasing the probability of its tunneling into the vacuum and, hence, the LDOS intensity. If the positive field is too high, then electrons can even become classically allowed in the vacuum region and field emission takes place (cf. Fig. 1). The electric field, affecting only evanescent tails of the surface state, actually changes the whole surface-state wave function including the part inside the crystal. This effect is demonstrated in Figs. 2(b) and 2(c) for the first vacuum layer and the topmost layer of the Cu(111) surface, respectively. For the latter, the total LDOS has a distinct shift around the energy of the surface-state band bottom. Note that the absolute values of the LDOS variations induced in the Cu layer are 2 orders larger than those in the second vacuum layer.

Field-induced modifications of the vacuum confining potential barrier can strongly affect the Fermi wavelength λ_F of the surface state. This can be achieved through changes in both the surface-state band bottom E_0 and the effective mass

TABLE I. Cu(111) surface-state parametrization, (1), at various strengths of the external field.

q (e)	Field (V/Å)	E_0 (eV)	k_F (Å^{-1})	$\lambda_F/2$ (Å)	m^* (m_e)
−0.31	−0.5	−0.457	0.221	14.22	0.408
0.0	0.0	−0.553	0.232	13.54	0.372
0.007	+0.1	−0.573	0.235	13.37	0.368
0.031	+0.5	−0.640	0.244	12.88	0.355

m^* of its electrons. Formally, λ_F can be expressed from the surface-state dispersion law:

$$E(k) = E_0 + (\hbar^2/2m^*)\,k^2. \quad (1)$$

Dispersion parameters were obtained by fitting our *ab initio* data to relation (1). To do this, we calculated spectral density maps $\mathcal{A}(\mathbf{k}_i, E_j)$ with momenta $\mathbf{k}_i$ aligned along the $\bar{\Gamma}$-$\bar{\mathrm{K}}$ section of the 2D BZ (cf. Fig. 1 in Ref. 40). Energies $\tilde{E}(\mathbf{k}_i)$ of the *ab initio* surface-state band were found by fitting $\mathcal{A}_{\mathbf{k}_i}(E_j)$ to the Lorentzian for each fixed $\mathbf{k}_i$. Then the *ab initio* band $\tilde{E}(\mathbf{k}_i)$ was fitted to dispersion law (1) by means of the least squares method. Results of the latter fitting are presented in Table I for several field strengths. The effective mass m^* exhibits a recognizable trend: the stronger the field-affected surface-state confinement, the higher the effective mass of the surface-state electrons. Despite the variable effective mass, the main changes in λ_F come from the field-induced shifts of the band bottom E_0. Variations of λ_F should manifest themselves in the alteration of surface-state standing wave patterns appearing around impurities[41] as demonstrated in Fig. 3. Surface-state-mediated long-range interaction[42] between adatoms on the Cu(111) surface should also be modified. Different positions of the first standing wave maximum imply the impact of the external field on the adatom scattering phase shift.

Field-induced changes in the surface-state binding energy were observed experimentally.[25,26] To make a link to experimental results by Kröger *et al.*,[26] we plot in Fig. 4 a shift of the surface-state band bottom as a function of the external field. The curve presented in Fig. 4 is in qualitative agreement with the experimental one, but we obtained a Stark shift with a milder slope. Presumably, the quantitative discrepancy appeared to be due to the semiempirical model applied to fit the experimental data.[26] The validity of our studies is

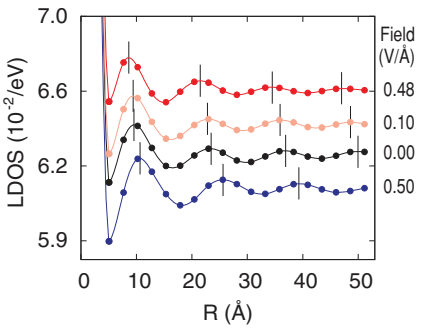

FIG. 3. (Color online) Standing waves around a Co adatom on Cu(111) calculated at the Fermi energy for different strengths of the external electric field.

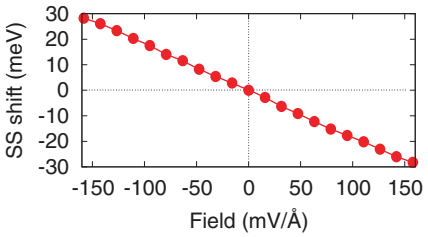

FIG. 4. (Color online) Shift of the Cu(111) surface-state band bottom as a function of the external electric field.

supported by *ab initio* results on field emission from a Ni(111) surface.[39] Dispersion laws of Ni(111) Shockley surface states were revealed in this work as a function of the applied field. The energy shifts obtained are the same as those shown in Fig. 4.

B. Spin-polarized surface states on a Co bilayer on Cu(111)

The next system we address is bilayer Co nanoislands grown on a Cu(111) substrate at room temperature.[43] STM/STS observations revealed two surface-related electronic states on Co nanoislands:[44] a strong localized peak 0.31 eV below E_F and a mainly unoccupied dispersive state, giving rise to quantum interference patterns of standing electron waves on Co islands. *Ab initio* calculations clarified that magnetic Co islands make surface states spin polarized.[44] The localized peak is of a minority character, while the dispersive state is the majority Shockley-type surface state. Properties of both states depend significantly on the exact structure of the Co nanoislands. In particular, energy positions of the localized minority peak are different on faulted and unfaulted Co islands by 0.07 eV.[45,46] Furthermore, it was revealed that minority surface-localized states are very sensitive to structural relaxations of Co nanoislands. Variations in island size can shift their energy by more than 0.1 eV.[46] The LDOS of the dispersive majority surface state also depends on the island size, but the mechanism in this case is related to the confinement of free-like majority electrons. Standing waves of the confined majority surface state cause spatial oscillation of spin polarization above the island. This effect was predicted theoretically[47] and confirmed experimentally.[48,49]

We apply our *ab initio* method to demonstrate the effect of the field on the energetics and magnetic properties of spin-polarized surface states on Co nanoislands. In these calculations, the Cu crystal was perturbed by six (111) layers of Cu, two unfaulted (or commensurate) layers of Co, nine layers of vacuum, and, again, Co and Cu layers. Extra charges were placed in the fifth vacuum layer. The Co bilayer changes the work function of the Cu(111) surface, so the critical value of the extra charge, at which field emission starts, is increased by $\Delta q = 0.0025\,e$, from $q_{\mathrm{Cu}} = 0.0375\,e$ up to $q_{2\mathrm{Co}} = 0.040\,e$. Variation $\Delta\Phi$ of the work function can be estimated as $\Delta\Phi = \beta\,\Delta q\,\Delta z$, where β is the slope of the *ab inito*–calculated dependence shown in Fig. 1, and $\Delta z = 8.85$ Å is the distance between external charges and the first vacuum layer. The obtained $\Delta\Phi = 0.33$ eV is very similar to the difference of 0.28 eV between work-functions $\Phi_{\mathrm{Cu}} \simeq 4.98$ eV and $\Phi_{\mathrm{Co}} \simeq 5.26$ eV of the Cu(111)[50] and the Co(0001)[51] surfaces, respectively.

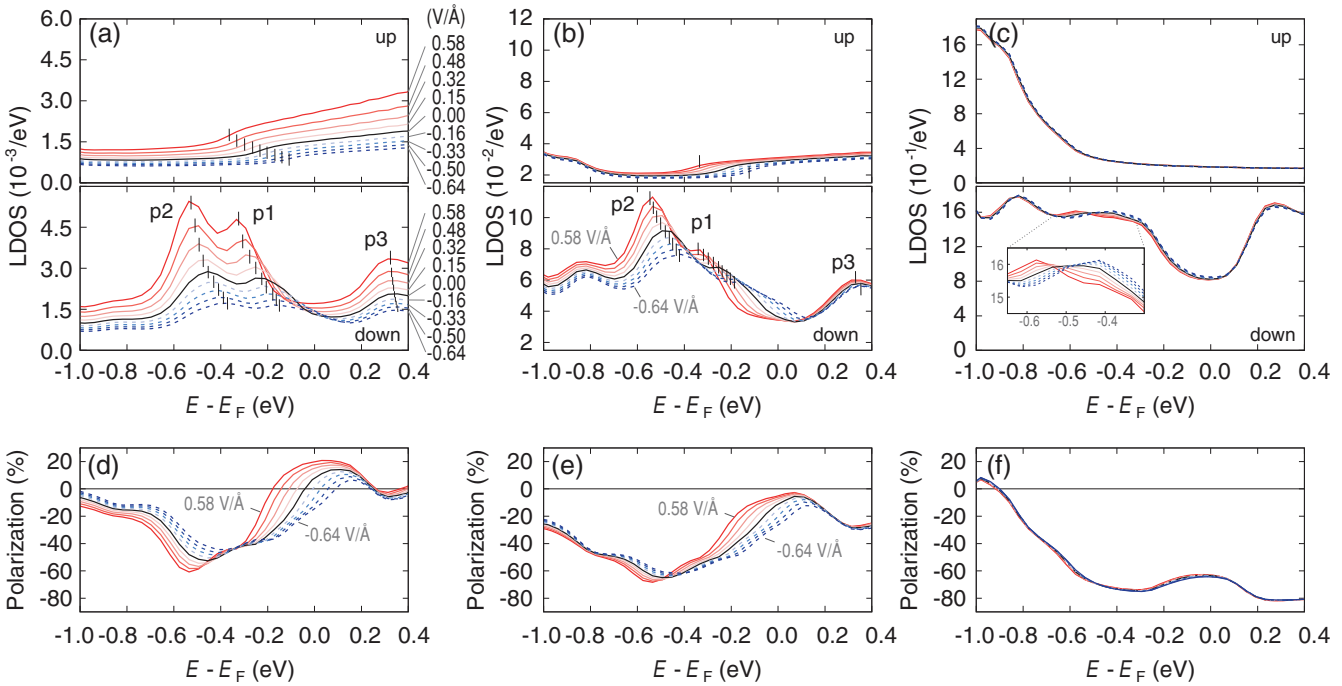

FIG. 5. (Color online) Spin-polarized LDOS calculated (a) at the second vacuum layer, at 4.16 Å above the surface; (b) at the first vacuum layer, at 2.08 Å; and (c) at the topmost Co layer. Layer alignment is the same as shown in Fig. 2(d). LDOS values obtained at positive, zero, and negative fields are plotted in (a–c) by light solid, black, and light dashed curves, respectively. In (a) and (b) the majority surface state (top) demonstrates a distinct onset with the bottom energy changing with the external electric field. Minority surface-related states (bottom) consist of three labeled peaks, whose energies depend on the external electric field. (d–f) Spin polarizations calculated from (a–c).

We start the presentation of our results on field-induced LDOS variations from the spin-polarized LDOS in the second vacuum layer situated at 4 Å above the Co bilayer. Majority and minority LDOS values are demonstrated in the top and bottom panels in Fig. 5(a). The majority surface state behaves like the surface state on the bare Cu(111) surface. Positive fields increase its density, simultaneously shifting the band bottom to lower energies. Negative fields, accordingly, decrease the density and shift the surface state upward. Positions of the band bottom are marked by thin vertical lines in Fig. 5(a). The overall shift of the majority surface-state band bottom is almost 0.3 eV.

Minority surface-related states on the Co bilayer have a rich structure. Three distinct peaks, labeled p1, p2, and p3, in Fig. 5(a) can be assigned.[46] Positions of peaks p1 and p2 are significantly affected by the external electric field. Depending on the field strength, peaks p1 and p2 can be found at energy intervals from -0.32 to -0.16 eV and from -0.52 to -0.38 eV, respectively. Peak p3, however, is very stable and exhibits a much smaller shift, by only 0.02 eV. Such a negligible response to the external electric field can appear because peak p3 is unoccupied and the corresponding electron density did not participate in the screening of the external field.

The ratio between majority ($\uparrow$) and minority ($\downarrow$) electrons is usually characterized in terms of the spin polarization defined as $P(E) = [\rho_\uparrow(E) - \rho_\downarrow(E)]/[\rho_\uparrow(E) + \rho_\downarrow(E)]$. The spin polarization calculated from data presented in Fig. 5(a) is presented in Fig. 5(d). According to our results, the external electric field creates a substantial change in the spin polarization near the Fermi level. The spin polarization, as follows from our calculations, can even change its sign, thus affecting the tunneling properties of the STM junction.[52–54] Significant variations in $P(E)$ actually appear due to a shift in peak p1. The drop in the minority LDOS in negative fields is compensated near the E_F by the approach of peak p1 to the Fermi level. As a result, a number of minority LDOS values have a narrow spot right below the E_F, as shown in the bottom panel in Fig. 5(d). Meanwhile, the majority LDOS exhibits significant changes in the same energy region. The spin polarization calculated from such states demonstrates spreading of values and even a reversal of the sign.

The sign of the spin polarization can be reversed only if the majority and the minority LDOS have approximately the same values. By example of the Cu(111) surface state, we learned that the surface state's density changes significantly, obeying the exponential decay law, as a function of the distance from the crystal-vacuum interface [cf. Figs. 2(a)–2(c)]. In the case of spin-polarized surface states, a height dependence of the spin polarization is, thus, predetermined by decay rates of majority and minority states. Spin-polarized LDOS values of the first vacuum layer and of the topmost Co atoms are presented in Figs. 5(b) and 5(c), respectively. The corresponding spin polarizations are shown in Figs. 5(f) and 5(g). The density of minority states becomes higher moving toward the surface. As a consequence, the spin polarization calculated at the first vacuum layer is negative over the whole energy range, but the field-induced spreading of the spin polarization values is still preserved near the E_F. The spin polarization of the topmost Co atoms is dominated by the minority d states. Although the external field induces significant variations in the

absolute values of the LDOS [cf. inset in Fig. 5(c)], the relative changes are hidden by the high density of Co d states and the external field only slightly changes the spin polarization of the Co bilayer and its magnetic moment.

The effect of the external electric field on the magnetism of the topmost Co layer can be quantified using the concept of the magnetoelectric coefficient. It has recently been demonstrated[21] that the induced surface magnetization ΔM of the magnetic Fe(001) surface can be assumed to be proportional to the applied electric field E,

$$\mu_0 \Delta M = \alpha_S E, \tag{2}$$

where α_S is the surface magnetoelectric coefficient. Fitting of our data to dependence (2) yielded values of $(1.28 \pm 0.04) \times 10^{-14}$ and $(-0.78 \pm 0.03) \times 10^{-14}$ G cm^2/V for magnetoelectric coefficients of the topmost and the second Co layers, respectively. Moduli of these values are similar to $\alpha_S^{001} = 2.9 \times 10^{-14}$ G cm^2/V reported for the Fe(001) surface.[21] The sign of the electric field in our work is opposite that used in Ref. 21. The prediction of Duan *et al.*[21] on the positive (in the notation of Ref. 21) sign of α_S is violated for the topmost layer of Co. This seeming contradiction appears because in our system the field-induced changes of the electronic density are maximal in the vacuum. Figure 5 clearly demonstrates that both *majority* and minority LDOS values are affected over a wide range of energies.

IV. CONCLUSIONS

In summary, we have presented an *ab initio* study of surface states exposed to an external electric field. We have focused on two well-known systems: the Shockley surface state on Cu(111) and spin-polarized surface states on a Co bilayer. Our results on the Shockley surface state on Cu(111) are in agreement with recent STS measurements.[26] We have demonstrated that the external field affects both the decay rate and the dispersion characteristics of the surface state. Being applied to spin-polarized surface states on the Co bilayer on Cu(111), our method has revealed significant modifications of both the majority and the minority surface-state counterparts. According to our results, the spin polarization can even change its sign.

*Corresponding author: stepanyu@mpi-halle.mpg.de

[1] G. Binnig, H. Rohrer, C. Gerber, and E. Weibel, Phys. Rev. Lett. **49**, 57 (1982).

[2] J. Tersoff and D. R. Hamann, Phys. Rev. B **31**, 805 (1985).

[3] D. M. Eigler and E. K. Schweizer, Nature **344**, 524 (1990).

[4] L. J. Whitman, Joseph A. Stroscio, R. A. Dragoset, and R. J. Celotta, Science **251**, 1206 (1991).

[5] J. A. Stroscio, L. J. Whitman, R. A. Dragoset, and R. J. Celotta, Nanotechnology **3**, 133 (1992).

[6] C. Girard, C. Joachim, C. Chavy, and P. Sautet, Surf. Sci. **282**, 400 (1993).

[7] R. S. Becker, J. A. Golovchenko, and B. S. Swartzentruber, Nature **325**, 419 (1987).

[8] I.-W. Lyo and P. Avouris, Science **253**, 173 (1991).

[9] Z.âH. Huang, M. Weimer, R. E. Allen, and H. Lim, J. Vac. Sci. Technol. A **10**, 974 (1992).

[10] L. Gerhard, T. K. Yamada, T. Balashov, A. F. Takács, R. J. H. Wesselink, M. Dne, M. Fechner, S. Ostanin, A. Ernst, I. Mertig, and W. Wulfhekel, Nature Nanotech. **5**, 792 (2010).

[11] Y. He, X. Y. Wei, C. T. Chan, and J. G. Che, Phys. Rev. B **71**, 045401 (2005).

[12] G. L. Kellogg, Phys. Rev. Lett. **70**, 1631 (1993).

[13] P. J. Feibelman, Phys. Rev. B **64**, 125403 (2001).

[14] K. Kunc and R. Resta, Phys. Rev. Lett. **51**, 686 (1983).

[15] J. Neugebauer and M. Scheffler, Surf. Sci. **287–288**, 572 (1993).

[16] H. Ness and A. J. Fisher, Phys. Rev. B **55**, 10081 (1997).

[17] Y. Sun, J. D. Burton, and E. Y. Tsymbal, Phys. Rev. B **81**, 064413 (2010).

[18] M. C. Troparevsky, K. Zhao, D. Xiao, Z. Zhang, and A. G. Eguiluz, Nano Lett. **9**, 4452 (2009).

[19] M. Weisheit, S. Fähler, A. Marty, Y. Souche, C. Poinsignon, and D. Givord, Science **315**, 349 (2007).

[20] S. J. Gamble, M. H. Burkhardt, A. Kashuba, R. Allenspach, S. S. P. Parkin, H. C. Siegmann, and J. Stöhr, Phys. Rev. Lett. **102**, 217201 (2009).

[21] C.-G. Duan, J. P. Velev, R. F. Sabirianov, Z. Zhu, J. Chu, S. S. Jaswal, and E. Y. Tsymbal, Phys. Rev. Lett. **101**, 137201 (2008).

[22] K. Nakamura, R. Shimabukuro, Y. Fujiwara, T. Akiyama, T. Ito, and A. J. Freeman, Phys. Rev. Lett. **102**, 187201 (2009).

[23] M. Tsujikawa and T. Oda, Phys. Rev. Lett. **102**, 247203 (2009).

[24] N. N. Negulyaev, V. S. Stepanyuk, W. Hergert, and J. Kirschner, Phys. Rev. Lett. **106**, 037202 (2011).

[25] L. Limot, T. Maroutian, P. Johansson, and R. Berndt, Phys. Rev. Lett. **91**, 196801 (2003).

[26] J. Kröger, L. Limot, H. Jensen, R. Berndt, and P. Johansson, Phys. Rev. B **70**, 033401 (2004).

[27] P. Wahl, M. A. Schneider, L. Diekhöner, R. Vogelgesang, and K. Kern, Phys. Rev. Lett. **91**, 106802 (2003).

[28] G. Kresse and J. Hafner, Phys. Rev. B **47**, 558 (1993); G. Kresse and J. Furthmüller, *ibid.* **54**, 11169 (1996).

[29] S. Heinze, X. Nie, S. Blügel, and M. Weinert, Chem. Phys. Lett. **315**, 167 (1999).

[30] J. Stahn, U. Pietsch, P. Blaha, and K. Schwarz, Phys. Rev. B **63**, 165205 (2001).

[31] P. Giannozzi, S. Baroni, N. Bonini, M. Calandra, R. Car, C. Cavazzoni, D. Ceresoli, G. L. Chiarotti, M. Cococcioni, I. Dabo *et al.*, J. Phys. Condens. Matter **21**, 395502 (2009).

[32] J. Zabloudil, R. Hammerling, L. Szunyogh, and P. Weinberger, *Electron Scattering in Solid Matter: A Theoretical and Computational Teatise, Springer Series in Solid-State Sciences,* Vol. 147 (Springer-Verlag, Berlin, 2005).

[33] K. Wildberger, V. S. Stepanyuk, P. Lang, R. Zeller, and P. H. Dederichs, Phys. Rev. Lett. **75**, 509 (1995).

[34] V. S. Stepanyuk, W. Hergert, K. Wildberger, R. Zeller, and P. H. Dederichs, Phys. Rev. B **53**, 2121 (1996).

[35] M. Otani and O. Sugino, Phys. Rev. B **73**, 115407 (2006).

[36] This definition is applied to make signs consistent with results of Kröger *et al.*[26]

[37] N. Memmel, Surf. Sci. Rep. **32**, 91 (1998).

[38]S. G. Davison and M. Steslicka, *Basic Theory of Surface States* (Clarendon Press, Oxford/Oxford University Press, New York, 1992).
[39]T. Ohwaki, D. Wortmann, H. Ishida, S. Blügel, and K. Terakura, Phys. Rev. B **73**, 235424 (2006).
[40]P. A. Ignatiev, N. N. Negulyaev, L. Niebergall, H. Hashemi, W. Hergert, and V. S. Stepanyuk, Phys. Status Solidi B **247**, 2537 (2010).
[41]M. F. Crommie, C. P. Lutz, and D. M. Eigler, Nature **363**, 524 (1993).
[42]V. S. Stepanyuk, A. N. Baranov, D. V. Tsivlin, W. Hergert, P. Bruno, N. Knorr, M. A. Schneider, and K. Kern, Phys. Rev. B **68**, 205410 (2003).
[43]N. N. Negulyaev, V. S. Stepanyuk, P. Bruno, L. Diekhoner, P. Wahl, and K. Kern, Phys. Rev. B **77**, 125437 (2008).
[44]L. Diekhöner, M. A. Schneider, A. N. Baranov, V. S. Stepanyuk, P. Bruno, and K. Kern, Phys. Rev. Lett. **90**, 236801 (2003).
[45]O. Pietzsch, A. Kubetzka, M. Bode, and R. Wiesendanger, Phys. Rev. Lett. **92**, 057202 (2004).
[46]M. V. Rastei, B. Heinrich, L. Limot, P. A. Ignatiev, V. S. Stepanyuk, P. Bruno, and J. P. Bucher, Phys. Rev. Lett. **99**, 246102 (2007).
[47]L. Niebergall, V. S. Stepanyuk, J. Berakdar, and P. Bruno, Phys. Rev. Lett. **96**, 127204 (2006).
[48]O. Pietzsch, S. Okatov, A. Kubetzka, M. Bode, S. Heinze, A. Lichtenstein, and R. Wiesendanger, Phys. Rev. Lett. **96**, 237203 (2006).
[49]H. Oka, P. A. Ignatiev, S. Wedekind, G. Rodary, L. Niebergall, V. S. Stepanyuk, D. Sander, and J. Kirschner, Science **327**, 843 (2010).
[50]H. B. Michaelson, J. Appl. Phys. **48**, 4729 (1977).
[51]S. Saito, K. Takeda, T. Soumura, M. Ohki, T. Tani, and T. Maeda, J. Appl. Phys. **71**, 5500 (1992).
[52]Y. Yayon, V. W. Brar, L. Senapati, S. C. Erwin, and M. F. Crommie, Phys. Rev. Lett. **99**, 067202 (2007).
[53]B. W. Heinrich, C. Iacovita, M. V. Rastei, L. Limot, J. P. Bucher, P. A. Ignatiev, V. S. Stepanyuk, and P. Bruno, Phys. Rev. B **79**, 113401 (2009).
[54]C. Iacovita, M. V. Rastei, B. W. Heinrich, T. Brumme, J. Kortus, L. Limot, and J. P. Bucher, Phys. Rev. Lett. **101**, 116602 (2008).